



HAL
open science

InsPecton of electron density maps supports wrongly modeled hexakisphosphate (InsP6) bound to African swine fever mRNA-decapping enzyme g5Rp

Marc Graille

► **To cite this version:**

Marc Graille. InsPecton of electron density maps supports wrongly modeled hexakisphosphate (InsP6) bound to African swine fever mRNA-decapping enzyme g5Rp. *Journal of Virology*, 2024, 98 (5), 10.1128/jvi.01597-23 . hal-04734987

HAL Id: hal-04734987

<https://cnrs.hal.science/hal-04734987v1>

Submitted on 14 Oct 2024

HAL is a multi-disciplinary open access archive for the deposit and dissemination of scientific research documents, whether they are published or not. The documents may come from teaching and research institutions in France or abroad, or from public or private research centers.

L'archive ouverte pluridisciplinaire **HAL**, est destinée au dépôt et à la diffusion de documents scientifiques de niveau recherche, publiés ou non, émanant des établissements d'enseignement et de recherche français ou étrangers, des laboratoires publics ou privés.

InsP₆ inspection of electron density maps supports wrongly modeled hexakisphosphate (InsP₆) bound to African swine fever mRNA-decapping enzyme g5Rp

Marc Graille¹

AUTHOR AFFILIATION See affiliation list on p. 3.

KEYWORDS crystal structure, viral decapping enzyme

In April 2022, a paper entitled “Structural Insight into Molecular Inhibitory Mechanism of InsP₆ on African Swine Fever Virus mRNA-Decapping Enzyme g5Rp” was published in the *Journal of Virology* (1). In this article, the authors focus on the g5Rp Nudix hydrolase from African swine fever virus (ASFV), the causative agent of swine infection. This enzyme is endowed with a diphosphoinositol polyphosphate (PP-InsP₅) phosphohydrolase activity converting PP-InsP₅ into inositol hexakisphosphate (InsP₆) as well as with a low mRNA-decapping activity (2–4). They also claim to have solved the crystal structure of g5Rp bound to the InsP₆ inhibitor at 2.25 Å resolution (PDB code: 7DNU). However, the 2Fo-Fc electron density map calculated from the experimental diffraction data does not match with InsP₆ (Fig. 1, compare panels A and B). Indeed, several InsP₆ atoms do not fit into the 2Fo-Fc electron density map and some phosphate groups fall within negative regions of the Fo-Fc difference map (Fig. 1A), indicating incorrect modeling of InsP₆. Additional observations further support this statement: (i) the mean B factor (148.4 Å²) for the modeled InsP₆ is very high compared to the mean B factor of all the g5Rp atoms (46.6 Å²); (ii) phosphate groups from symmetry-related InsP₆ molecules are located less than 3 Å from each other (Fig. 1A), which is energetically highly unfavorable; (iii) the side chain of positively charged Lys residues (K8 and K133) are modeled so as to form strong electrostatic interactions with negatively charged InsP₆ phosphate groups but are not defined by electron density, indicating that these side chains are in fact highly flexible, which should not be the case due to their assumed roles in InsP₆ binding; and (iv) the Fo-Fc omit difference map calculated in the absence of InsP₆ bound to g5Rp model also fails to confirm the presence of InsP₆ in this region of g5R (Fig. 1C and D). This latter Fo-Fc difference omit map suggests the presence of a yet to be identified ligand, different from InsP₆ and which could originate from the buffers used during protein purification (unfortunately not indicated in the Materials and Methods of the article) or which could have been co-purified with g5Rp as frequently observed in crystal structures (5–7). This incorrect structure does not call into question most of the experimental results obtained by biochemical methods. However, I believe it is important to alert the scientific community about this error, so that this structure is not used as a basis for future research aimed, for example, at trying to develop anti-ASFV drugs on the basis of this incorrect structural information. The authors of this crystal structure should also be encouraged to correct it and publish an erratum in the *Journal of Virology*, as suggested for other similar problems (8).

The great advantage of X-ray crystallographic structures over molecular docking models is that the former generate models based on experimental diffraction data. In recent years, more and more tools have been developed to identify ligands corresponding to Fo-Fc difference maps and thus help X-ray crystallographers identify molecules

Editor Felicia Goodrum, The University of Arizona, Tucson, Arizona, USA

Address correspondence to Marc Graille, marc.graille@polytechnique.edu.

The author declares no conflict of interest.

Ed. Note: The authors of the original article did not respond at the time of publication.

See the original article at <https://doi.org/10.1128/jvi.01905-21>.

Published 24 April 2024

Copyright © 2024 American Society for Microbiology. All Rights Reserved.

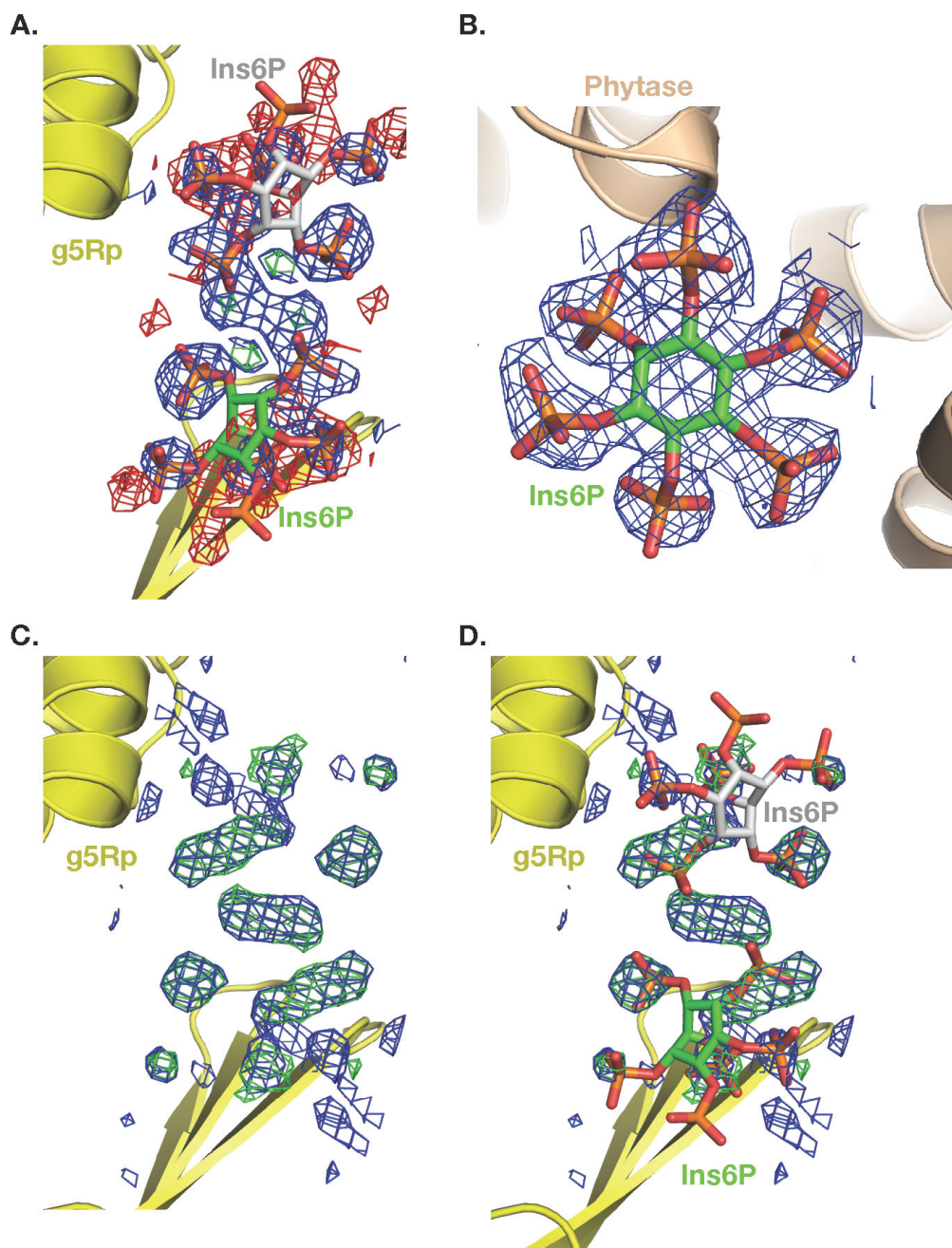


FIG 1 Electron density maps illustrating the incorrect modeling of InsP6. (A) 2Fo-Fc (contoured at 1 σ ; blue) and Fo-Fc [contoured at -3σ (red) or 3 σ (green)] electron density maps available from the Protein Data Bank [<http://www.rcsb.org/>; (9)] for the PDB entry 7DNU (1). The g5Rp protein is colored in yellow. The carbon atoms of InsP6 bound to g5Rp and of its symmetrical mate are colored in green and gray, respectively. Phosphorus and oxygen atoms are colored orange and red, respectively. All panels of this figure were generated using the Pymol software (10). This color code and the map contouring levels are used in all panels. (B) Illustration of the 2Fo-Fc electron density map of InsP6 bound to *Escherichia coli* phytase [wheat; (11)], which was determined at a similar resolution (2.28 Å vs 2.25 Å for PDB entry 7DNU). The coordinates and electron density map were downloaded from the Protein Data Bank [<http://www.rcsb.org/>; (9)]. (C) 2Fo-Fc and Fo-Fc electron density maps calculated by the PHENIX.REFINE software in the absence of InsP6 bound to g5Rp (12). (D) Same as C, except that the InsP6 modeled by the authors are shown as sticks, showing a complete discrepancy between the shape of the electron density omit maps and the structure of InsP6.

bound to crystallized proteins (13, 14). These tools complement human expertise in electron density map analysis to help scientists avoid over-interpreting electron density maps. X-ray crystallographers need to be particularly attentive to this type of situation, as students or scientists with no expertise in structural biology may simply consider that since these results have been published in peer-reviewed journals, they are correct.

AUTHOR AFFILIATION

¹Laboratoire de Biologie Structurale de la Cellule (BIOC), CNRS, École polytechnique, Institut Polytechnique de Paris, Palaiseau, France

AUTHOR ORCID*s*

Marc Graille  <http://orcid.org/0000-0002-7853-5852>

AUTHOR CONTRIBUTIONS

Marc Graille, Writing – review and editing

REFERENCES

- Yang Y, Zhang C, Li X, Li L, Chen Y, Yang X, Zhao Y, Chen C, Wang W, Zhong Z, Yang C, Huang Z, Su D. 2022. Structural insight into molecular inhibitory mechanism of Insp(6) on African swine fever virus mRNA-decapping enzyme g5Rp. *J Virol* 96:e01905-21. <https://doi.org/10.1128/jvi.01905-21>
- Cartwright JL, Safrany ST, Dixon LK, Darzynkiewicz E, Stepinski J, Burke R, McLennan AG. 2002. The g5R (D250) gene of African swine fever virus encodes a nudix hydrolase that preferentially degrades diphosphoinositol polyphosphates. *J Virol* 76:1415–1421. <https://doi.org/10.1128/jvi.76.3.1415-1421.2002>
- Parrish S, Hurchalla M, Liu SW, Moss B. 2009. The African swine fever virus g5R protein possesses mRNA decapping activity. *Virology* 393:177–182. <https://doi.org/10.1016/j.virol.2009.07.026>
- Quintas A, Perez-Nunez D, Sanchez EG, Nogal ML, Hentze MW, Castello A, Revilla Y. 2017. Characterization of the African swine fever virus decapping enzyme during infection. *J Virol* 91:e00990-17. <https://doi.org/10.1128/JVI.00990-17>
- Stehlin C, Wurtz JM, Steinmetz A, Greiner E, Schule R, Moras D, Renaud JP. 2001. X-ray structure of the orphan nuclear receptor RORbeta ligand-binding domain in the active conformation. *EMBO J* 20:5822–5831. <https://doi.org/10.1093/emboj/20.21.5822>
- Frenois F, Engohang-Ndong J, Lochet C, Baulard AR, Villeret V. 2004. Structure of EthR in a ligand bound conformation reveals therapeutic perspectives against tuberculosis. *Mol Cell* 16:301–307. <https://doi.org/10.1016/j.molcel.2004.09.020>
- Gokulan K, O'Leary SE, Russell WK, Russell DH, Lalgondar M, Begley TP, Ioerger TR, Sacchettini JC. 2013. Crystal structure of *Mycobacterium tuberculosis* polyketide synthase 11 (PKS11) reveals intermediates in the synthesis of methyl-branched alkylpyrones. *J Biol Chem* 288:16484–16494. <https://doi.org/10.1074/jbc.M113.468892>
- Wlodawer A, Dauter Z, Porebski PJ, Minor W, Stanfield R, Jaskolski M, Pozharski E, Weichenberger CX, Rupp B. 2018. Detect, correct, retract: how to manage incorrect structural models. *FEBS J* 285:444–466. <https://doi.org/10.1111/febs.14320>
- Berman HM, Westbrook J, Feng Z, Gilliland G, Bhat TN, Weissig H, Shindyalov IN, Bourne PE. 2000. The protein data bank. *Nucleic Acids Res* 28:235–242. <https://doi.org/10.1093/nar/28.1.235>
- Schrodinger L. n.d. The pymol molecular graphics system, version 2.4.2
- Lim D, Golovan S, Forsberg CW, Jia Z. 2000. Crystal structures of *Escherichia coli* phytase and its complex with phytate. *Nat Struct Biol* 7:108–113. <https://doi.org/10.1038/72371>
- Afonine PV, Grosse-Kunstleve RW, Echols N, Headd JJ, Moriarty NW, Mustyakimov M, Terwilliger TC, Urzhumtsev A, Zwart PH, Adams PD. 2012. Towards automated Crystallographic structure refinement with Phenix.Refine. *Acta Crystallogr D Biol Crystallogr* 68:352–367. <https://doi.org/10.1107/S0907444912001308>
- Binkowski TA, Cuff M, Nocek B, Chang C, Joachimiak A. 2010. Assisted assignment of ligands corresponding to unknown electron density. *J Struct Funct Genomics* 11:21–30. <https://doi.org/10.1007/s10969-010-9078-7>
- Kowiel M, Brzezinski D, Porebski PJ, Shabalin IG, Jaskolski M, Minor W. 2019. Automatic recognition of ligands in electron density by machine learning. *Bioinformatics* 35:452–461. <https://doi.org/10.1093/bioinformatics/bty626>